Incorporation of Free Halide Ions Stabilizes Metal–Organic Frameworks (MOFs) Against Pore Collapse and Renders Large-pore Zr-MOFs Functional for Water Harvesting

Journal:	*Journal of Materials Chemistry A*
Manuscript ID	TA-COM-11-2021-010217.R1
Article Type:	Communication
Date Submitted by the Author:	30-Jan-2022
Complete List of Authors:	Lu, Zhiyong; Hohai University, College of Mechanics and Materials; Northwestern University, Department of Chemistry Duan, Jiaxin; Northwestern University, Department of Chemistry Du, Liting; Nanjing Forestry University, Advanced Analysis and Testing Center Liu, Qin; Northwestern University, Department of Chemistry; University of Science and Technology of China, National Synchrotron Radiation Lab Schweitzer, Neil; Northwestern University, Center for Catalysis and Surface Science; Argonne National Laboratory, Chemical Science and Engineering Division Hupp, Joseph; Northwestern University, Department of Chemistry

SCHOLARONE™
Manuscripts

COMMUNICATION

Incorporation of Free Halide Ions Stabilizes Metal–Organic Frameworks (MOFs) Against Pore Collapse and Renders Large-pore Zr-MOFs Functional for Water Harvesting

Zhiyong Lu,*[a,b,†] Jiaxin Duan,[b,†] Liting Du,[c] Qin Liu,[b] Neil Schweitzer[d] and Joseph T. Hupp*[b]

Chemically and hydrolytically stable MOFs have shown promising water-vapor adsorption properties. However, MOFs that can simultaneously satisfy the following three requirements for effective water harvesting from low-humidity air are quite rare: 1) high water-uptake capacity; 2) hydrolytic and mechanical stability; 3) complete uptake at ~20-30% relative humidity (RH). Here we show that incorporating free halide ions is effective for enabling a representative Zr-MOF to meet these requirements for water harvesting. As-synthesized MOF-808 initially exhibits very good capacity at RH≥30%, but quickly suffers large capacity losses due to water-evacuation-induced pore collapse. Via a framework-charging and free counter-ion inclusion approach, we were able to replace node-ligated formate anions with charge-neutral aqua ligands and site desired water-sorbing free-halide ions within the large pores of MOF-808. Altered samples show increased gravimetric water uptake, show beneficial shifts of water sorption isotherms toward lower water-vapor partial pressure, eliminate undesirable sorption/desorption isotherm hysteresis, and render MOF-808-Br indefinitely recyclable for ambient-temperature uptake of water vapor and lower-temperature liquid-water release.

Porous materials, such as metal–organic frameworks (MOFs), have shown promising water-vapor adsorption properties that are relevant for many applications (*e.g.*, heat pumps, chillers, humidity control, hydrolytic catalysis, water harvesting from air) depending on the relative humidity (RH) where uptake occurs.[1-12] Chemical and mechanical hydrolytic stability of MOFs in the presence of water,[2,5,13-17] and during water removal, are

prerequisites for these applications.[18] For water-harvesting from air, humidity is spontaneously captured from air, and condensed as liquid water within interior nanostructured pores of the crystalline MOF. A change in external relative humidity, typically engendered by a modest change in temperature (for example, night versus day), ideally causes the MOF to release the captured water, setting the stage for additional vapor-capture/water-release cycles.[6,7,19-21]

Materials for harvesting water from air of low or moderate humidity will basically exhibit: 1) a high water-uptake capacity (typically achieved by relying on comparatively large pores (*e.g.*, a few nanometers in diameter)),[1,6,16] 2) chemical hydrolytic stability during water-vapor uptake and mechanical stability (for example, against pore-collapsing capillary forces) during water release (typically achieved by comparatively small pores, together with water-substitution-resistant bonds between MOF nodes and organic linkers),[3,6,13,22] and 3) depending on the application, complete or nearly complete uptake of water vapor and reversible storage as liquid water, at or near 20% relative humidity (typically achieved by relying on comparatively small pores (*e.g.*, diameters of ~1 nm or less)).[1,6,22] The extant literature points to inherent contradictions in MOF architecture optimization for these three sets of behavior. Oversimplifying, large pores are desirable for meeting requirement 1, while small pores are desirable for satisfying requirements 2 and 3.[4,22,23] As such, very few examples exist of MOFs that can simultaneously satisfy all three requirements.[1,6,7,16,24]

Herein, we show that certain large-pore, high-water-capacity MOFs generally satisfying requirement 1 can be rendered effective in simultaneously satisfying requirements 2 and 3. MOFs typically are charge-neutral. Chemically imparting a net electrical charge to a framework, and simultaneously incorporating water-soluble ions of opposite charge into MOF pores, such that the ions retain freedom of motion through incorporated liquid-water, and are not chemically grafted or otherwise strongly bound to the charged framework, leads to the desired behavior. This behavior includes enhanced retention of high uptake capacity across multiple water uptake

[a.] *College of Mechanics and Materials, Hohai University, Nanjing 210098, China Email: johnlook1987@gmail.com.*

[b.] *Department of Chemistry, Northwestern University, 2145 Sheridan Road, Evanston, Illinois 60208, USA. Email: j-hupp@northwestern.edu*

[c.] *Advanced Analysis and Testing Center, Nanjing Forestry University, Nanjing 210037, China.*

[d.] *Department of Chemical Engineering, Northwestern University, 2145 Sheridan Road, Evanston, Illinois 60208, USA.*

† Z.L. and J.D. contributed equally.

and release cycles, and sharp, reversible uptake at substantially lower relative humidity than otherwise achieved.[25]

As a target MOF for halide ion incorporation and pore stabilization, we selected one of the widely most used Zr-MOFs, **MOF-808**.[1] (Note that **MOF-808** is synthesized by using formic acid as modulator; in its as-synthesized form, hereafter termed **MOF-808-Formate**, each Zr_6 node of the MOF is connected with six tri-benzenecarboxylates and theoretically capped with six formates (however, see below)). Broadly consistent with earlier reports,[1] Figure 1a shows that **MOF-808-Formate** initially exhibits very good H_2O uptake (~840 $cm^3 \cdot g^{-1}$), with uptake being sharp and largely complete (~760 $cm^3 \cdot g^{-1}$) at a saturation-normalized partial pressure for water, P/P_0, of ~0.38 (38% RH). The plot for water desorption/release retraces the adsorption/uptake plot down to about 300 $cm^3 \cdot g^{-1}$ ($P/P_0 \leq 0.28$), with the plots only re-converging below P/P_0=0.04. Starting with the second cycle, however, water uptake is greatly decreased, reaching only ~290 $cm^3 \cdot g^{-1}$ at the isotherm plateau, $P/P_0 \cong 0.31$, and ~380 $cm^3 \cdot g^{-1}$ near saturation, *i.e.* P/P_0=0.9.
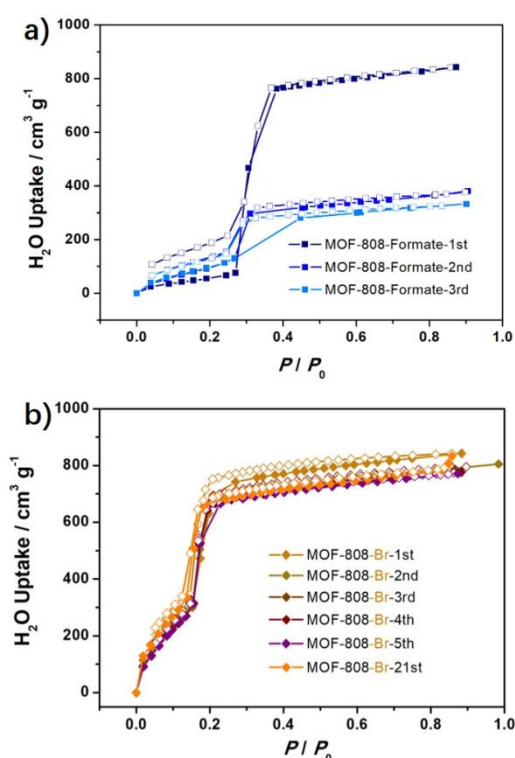

Figure 1. Isotherms for water uptake and release by: a) **MOF-808-Formate**, 3 cycles; b) **MOF-808-Br**, cycles 1-5 and 21.

Water-filled or -nearly-filled MOFs, including otherwise robust zirconium-based MOFs, are known to be susceptible to pore collapse during evacuation, where collapse is driven by capillary forces rather than hydrolysis effects.[13,26] These forces increase with increasing condensed-phase surface tension. Liquid-water's surface tension is unusually large and, thus, its removal from pores is accompanied by large mechanical stresses. Susceptibility to pore collapse generally increases with pore size; for **MOF-808** the pore diameter is 1.84 nm, *i.e.* just below mesopore size and slightly below the size threshold (~2.0 nm) for capillary-induced hysteresis behavior for water.[7,26,27] The

striking capacity loss in Figure 1a is consistent with irreversible pore collapse – a notion supported by observation of decreased porosity and crystallinity (Figure S4-5).

While capacity loss has obvious and direct implications for water-harvesting, it also has implications for pore-governed (or potentially governed) problems such as guest-molecule transport dynamics, chemical separations, and chemical catalysis. Notice that for water in **MOF-808-Formate**, pore occupancy sharply increases up to ~38% relative humidity and, for desorption, sharply decreases down to ~28% relative humidity (RH). This, presumably, is the RH range over which pore-collapse is manifest. To the extent that RH ranges encountered in nominally climate-controlled labs extend beyond the above-mentioned upper (38%) and lower (28%) bounds, "dry" **MOF-808** samples exposed to these variations would experience pore-collapse even before being deployed for water-harvesting, chemical separations, chemical storage, or catalysis.
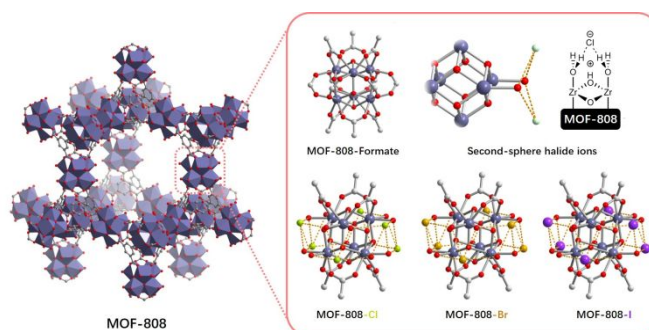

Figure 2. Proposed siting of charge-compensating halide ions in **MOF-808** after each of several nonstructural anionic formate ligands has been replaced by a pair of charge-neutral aqua ligands. Replacement renders the overall framework cationic. Proposed siting is informed by SCXRD data for **NU-1000-Cl**.[14]

For a close-related mesoporous, eight-connected Zr-MOF, **NU-1000**, we recently found that: a) standard protocols for removal of synthesis modulators, such as benzoate, introduce in their place as nonstructural node ligands, adventitiously formed formate,[14,28] b) these difficult-to-detect ligands can inhibit node-based catalytic activity, interfere with post-synthetic node-functionalization,[14,29] and behave as unintended chemical reductants toward subsequently installed metal ions such as Cu^{2+},[30] c) unwanted formate ligands can be removed and replaced with pairs of node-sited aqua ligands, together with charge-compensating, but non-ligated, halide ions, via treatment of the formate-afflicted MOF with a solution of dioxane + aqueous HCl,[14,31] HBr, or HI, and d) if left untreated, but submerged in water overnight, each formate is replaced by a terminal aqua & hydroxo ligand pair.[32] A single-crystal X-ray diffraction (SCXRD) structure for water-filled and HCl-treated **NU-1000**, showed that chloride ions (~4/node) are sited in the node's second-sphere, rather being directly grafted to the node. The structure also shows that each chloride is hydrogen-bonded by two node-attached aqua ligands.[14] Similar SCXRD results,

regarding halide-ion siting, have been reported for the Zr-MOF, DUT-67.[33]

We reasoned that similar behavior (*i.e.*, formate replacement with terminal aqua ligand pairs), and similar hydrogen-bonding interactions with free halide ions, would obtain for halo-acid treated **MOF-808** (Figure 2). With terminal aqua ligands being gone, activated halo-loaded MOF-808s were expected to show higher initial uptakes than MOF-808-Formate with formate ligands coordinated to the node. We further reasoned that the hydrogen-bonding interactions with free halide ions might decrease the affinity of pore-filling water molecules for MOF pore walls – particularly at the nodes – by blocking hydrogen-bonding of added water molecules to node aqua ligands, thereby diminishing capillary-force-based stressing of the framework during water evacuation and potentially eliminating subsequent MOF pore collapse.

Consistent with unwanted pore-collapse, Figure 1a shows that the high initial water uptake capacity of **MOF-808-Formate**, (762 $cm^3 \cdot g^{-1}$ at the plateau at P/P_0=0.38), fades rapidly – yielding only ~275 $cm^3 \cdot g^{-1}$ for cycle 3. In striking contrast (Figure 1b) is the highly resilient behavior of **MOF-808-Br** (HBr-treated **MOF-808**).[34] Plots for cycles 1-5 and 21 evince that: a) the magnitude of water uptake by **MOF-808-Br** in the first sorption cycle is similar to that for **MOF-808-Formate** at both the onset of the isotherm plateau (752 $cm^3 \cdot g^{-1}$) and near saturation (861 $cm^3 \cdot g^{-1}$; P/P_0=0.9), despite 145% greater formula weight; b) uptake and release are sharper, *i.e.* occur over a narrower RH (normalized pressure) range, which is consistent with pore-

condensation type water-vapor uptake, at least for the steepest segment of the isotherms; c) the median point for water sorption/desorption is pushed from P/P_0=0.3 for **MOF-808-Formate** to P/P_0=0.2 for **MOF-808-Br**; d) sorption occurs over two distinct regions of pressure, but, essentially zero hysteresis is registered, e) th*e second and subsequent sorption cycles register almost no capacity decrease* relative to the first, illustrating that porosity is maintained and capillary-force-induced pore collapse is absent. PXRD plots for **MOF-808-Br** before water-vapor exposure and after 21 uptake & release cycles – measurements spanning ten days of assessment, without interruption – are nearly identical, and closely match those for **MOF-808-Formate** *prior* to water uptake (Figures 3, S5), *i.e.* **MOF-808-Br**'s crystallinity for doesn't degrade.

NMR data (Figure S2) for digested **MOF-808-Formate** shows the presence of 4.0±0.2 of an anticipated 6 formate ligands per Zr_6 node. Ambient-temperature treatment with aq. HBr in dioxane eliminates NMR-detectable formate and installs 3.5±0.2 Br^-/node (Figure S18). Analogous treatments with aq. HCl in dioxane similarly eliminate NMR-detectable formate (Figure S9) and install 3.5±0.2 Cl^-/Zr_6 node (Figure S7-8) as measured by SEM-EDS of chlorine and zirconium with intact crystallites. In contrast to HCl and HBr, aq. HI in dioxane is only partially effective in removing formate and installing iodide. Increasing the concentration of HI and the number of washing steps did not afford completely formate-free samples. Thus, **MOF-808-I** retains 0.56±0.2 formate/node (Figure S28) and contains only 2.3±0.1 iodides (Figure S27).
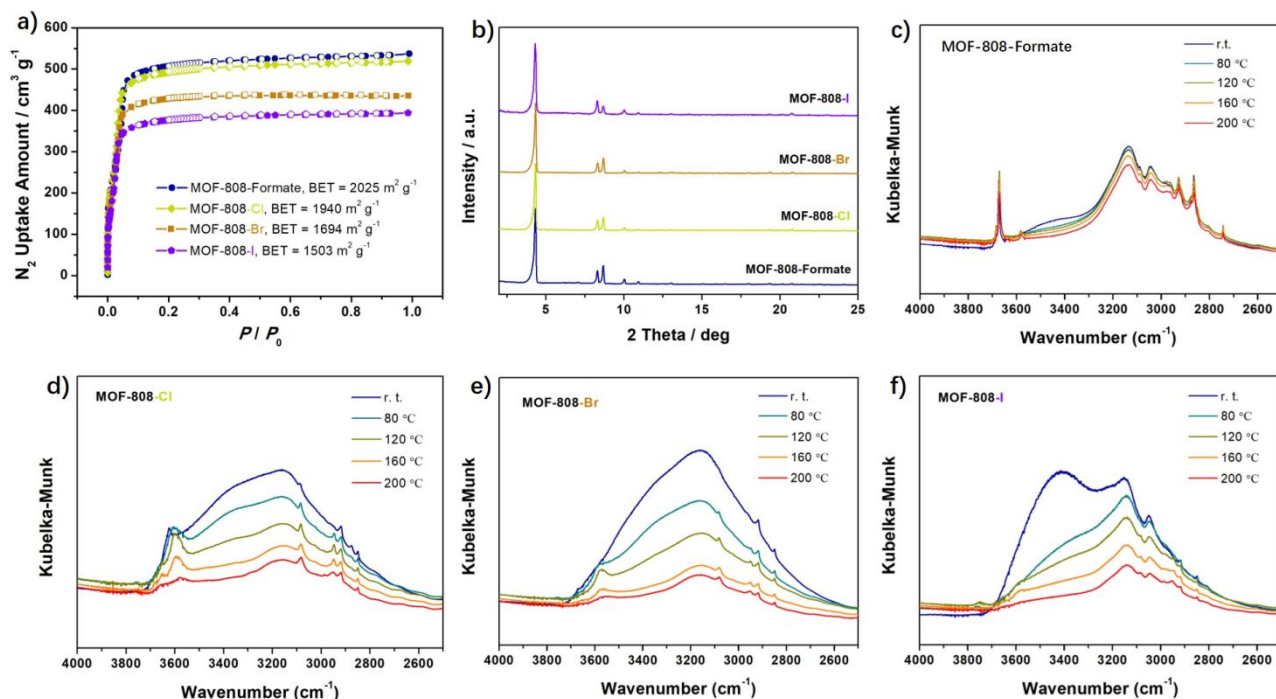

Figure 3. N$_2$ (77K) isotherms a) and PXRD patterns b) for the **MOF-808** series; c), d), e) and f) are DRIFTS spectra for members of the series, recorded at progressively higher temperatures under flowing argon.

From N_2 isotherms (77K; Figure 3a), BET surface areas for **MOF-808-Cl**, **MOF-808-Br**, and **MOF-808-I** are 1940, 1690, and 1500 m²•g⁻¹, respectively. The lower gravimetric areas of **MOF-808-Br** and **MOF-808-I** are broadly consistent with 1.4-1.5-fold greater formula weights for, relative to the as-synthesized framework. Pore-size distributions show slight decreases in width (Figure S40).

Shown in Figure 3c-f are variable-temperature DRIFT spectra in the O-H stretch region for water for each of four **MOF-808** variants, following ten-minute exposures to lab air (~30% RH). Halide-containing samples (Figure 3d-f) display a broad peak (~3000 and 3600 cm⁻¹) for weakly sorbed water, that is lost with temperature elevation. **MOF-808-Formate** (Figure 3c), in contrast, displays only a small amount of optical density ascribable to weakly sorbed water. We interpret the behavior as evidence for halide ions,[6,27] but not formate, sequestering multiple water molecules and removing them from participation in the pore-filling water clusters responsible for pore-collapse-inducing, capillary-force effects during water evacuation. Further, the results suggest that formate is released only after extended exposure to liquid or near-liquid water.

The completion of condensation-type pore filling at RHs as low as ~22% suggests that substantial water harvesting may be

Figure 4a compares 1st cycle water isotherms for **MOF-808-Formate**, **MOF-808-Cl**, **MOF-808-Br**, and **MOF-808-I**, and shows that the lightest halide engenders the highest gravimetric uptake. MOF-to-MOF comparisons are often made at P/P_0=0.3. On this basis, uptake by **MOF-808-Cl** (802 cm³•g⁻¹; 0.65 g•g⁻¹) is roughly double that of **MOF-808-Formate**, largely reflecting the much lower partial pressure for needed for condensation-type pore-filling of the former. To our knowledge, only values for **Co₂Cl₂BTDD**[7] and **Ni₂Cl₂BTDD**[7] are greater (Table S2).

Equally as gravimetric uptakes, volumetric assessments are also meaningful for water-harvesting (Figure 4b).[35] Here **MOF-808-Br** significantly surpasses both **MOF-808-Cl** and **MOF-808-Formate**, reaching 1033 cm³•cm⁻³ at P/P_0=0.9. To our knowledge, this is a record high experimental value among all reported water-sorbing MOFs (Table S1).

To evaluate the potential of **MOF-808-Br** to generate potable water in desert regions, day/night temperatures and RH values typical of the Arabian[1] and Sonoran[36] deserts were simulated, *i.e.* 45 °C, 5% RH (day) and 25 °C, 35% RH (night). Figure 4 shows full isotherms on absolute humidity (panel c) and relative humidity (panel d) scales. From the plots, the working capacity is 600 cm³g⁻¹ (0.48 g•g⁻¹), a value apparently exceeded only by **Ni₂Cl₂BTDD** (0.86 g•g⁻¹),[7] **Co₂Cl₂BTDD** (0.82 g•g⁻¹),[7] and **MOF-808-Cl** (0.53 g•g⁻¹; 1st cycle).

MOF-808-Br, respectively, are working capacities of 0.41 and 0.38 g•g⁻¹ – record high values for these conditions.
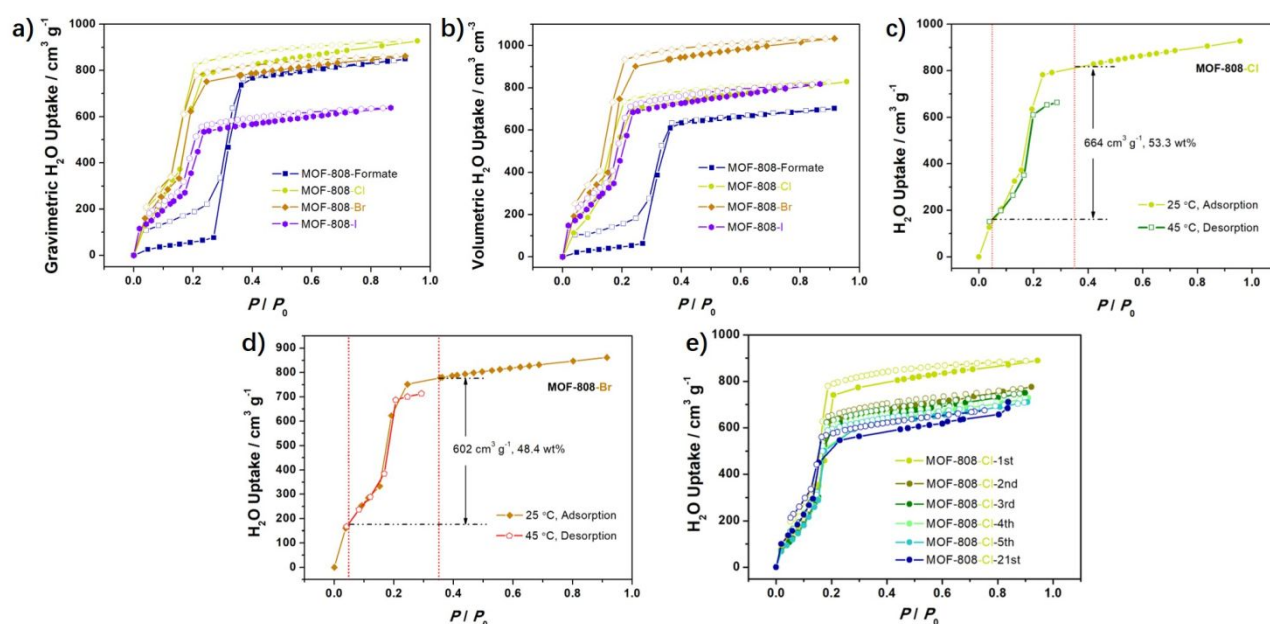

Figure 4. a) and b) gravimetric and volumetric water isotherms for **MOF-808** series at 25 °C; c) and d) assessment of **MOF-808-Br**'s 1st cycle deliverable capacity on absolute and relative humidity scales, under following simulated desert conditions: 45 °C, 5% RH (day), and 25 °C, 35% RH (night); e) repetitive cycling for **MOF-808-Cl,** cycles 1-5 and 21.

possible even in inland deserts, such as the Taklimakan desert (northwestern China; typical conditions: 45 °C, 5% RH (day), and 25 °C, 20% RH (night)).[37] Calculated for **MOF-808-Cl** and

Conclusions

In summary, we demonstrated a new approach of framework charging together with permanent incorporation of non-ligated halide ions that can stabilize large-pore Zr-MOF against catastrophic, water-evacuation-induced, pore collapse – in turn, rendering it very promising gravimetrically and outstanding volumetrically for repetitive water harvesting from low-humidity air. The pristine MOF-808 exhibits very good capacity at RH≥30%, but quickly suffers large capacity losses due to water-evacuation-induced pore collapse. Through this new approach, we are able to graft different non-ligated halide ions in MOF-808. Compared with the formate-bonded version of MOF-808, the halide-ion-loaded samples not only show an increase of water uptake capacity, but a shift of the steep of isotherms towards lower partial pressure within the water-harvesting range. Moreover, the cycling stability of MOF-808 was significantly strengthened, which renders MOF-808-Br indefinitely recyclable for ambient-temperature uptake of water vapor and lower-temperature liquid-water release. This approach provides new insight into the optimization of MOFs' water adsorption property and further results/consequences for other applications and other MOFs will be reported in due course.

Conflicts of interest

There are no conflicts to declare.

Acknowledgement

References

1. H. Furukawa, F. Gandara, Y. B. Zhang, J. Jiang, W. L. Queen, M. R. Hudson and O. M. Yaghi, *J Am Chem Soc*, 2014, **136**, 4369-4381.
2. N. C. Burtch, H. Jasuja and K. S. Walton, *Chem Rev*, 2014, **114**, 10575-10612.
3. P. Deria, Y. G. Chung, R. Q. Snurr, J. T. Hupp and O. K. Farha, *Chem Sci*, 2015, **6**, 5172-5176.
4. A. Khutia, H. U. Rammelberg, T. Schmidt, S. Henninger and C. Janiak, *Chem Mater*, 2013, **25**, 790-798.
5. X. L. Lv, S. Yuan, L. H. Xie, H. F. Darke, Y. Chen, T. He, C. Dong, B. Wang, Y. Z. Zhang, J. R. Li and H. C. Zhou, *J Am Chem Soc*, 2019, **141**, 10283-10293.
6. A. J. Rieth, A. M. Wright, G. Skorupskii, J. L. Mancuso, C. H. Hendon and M. Dinca, *J Am Chem Soc*, 2019, **141**, 13858-13866.
7. A. J. Rieth, S. Yang, E. N. Wang and M. Dinca, *ACS Cent Sci*, 2017, **3**, 668-672.
8. S. M. Towsif Abtab, D. Alezi, P. M. Bhatt, A. Shkurenko, Y. Belmabkhout, H. Aggarwal, Ł. J. Weseliński, N. Alsadun, U. Samin, M. N. Hedhili and M. Eddaoudi, *Chem*, 2018, **4**, 94-105.
9. J. Zheng, R. S. Vemuri, L. Estevez, P. K. Koech, T. Varga, D. M. Camaioni, T. A. Blake, B. P. McGrail and R. K. Motkuri, *J Am Chem Soc*, 2017, **139**, 10601-10604.
10. R. G. AbdulHalim, P. M. Bhatt, Y. Belmabkhout, A. Shkurenko, K. Adil, L. J. Barbour and M. Eddaoudi, *J Am Chem Soc*, 2017, **139**, 10715-10722.
11. D. Lenzen, J. G. Eggebrecht, P. G. M. Mileo, D. Frohlich, S. Henninger, C. Atzori, F. Bonino, A. Lieb, G. Maurin and N. Stock, *Chem Commun*, 2020, **56**, 9628-9631.
12. Z. Lu, L. Du, R. Guo, G. Zhang, J. Duan, J. Zhang, L. Han, J. Bai and J. T. Hupp, *J Am Chem Soc*, 2021, **143**, 17942–17946.
13. J. E. Mondloch, M. J. Katz, N. Planas, D. Semrouni, L. Gagliardi, J. T. Hupp and O. K. Farha, *Chem Commun*, 2014, **50**, 8944-8946.
14. Z. Lu, J. Liu, X. Zhang, Y. Liao, R. Wang, K. Zhang, J. Lyu, O. K. Farha and J. T. Hupp, *J Am Chem Soc*, 2020, **142**, 21110-21121.
15. Z. Lu, R. Wang, Y. Liao, O. K. Farha, W. Bi, T. R. Sheridan, K. Zhang, J. Duan, J. Liu and J. T. Hupp, *Chem Commun*, 2021, **57**, 3571-3574.
16. D. Lenzen, J. Zhao, S. J. Ernst, M. Wahiduzzaman, A. Ken Inge, D. Frohlich, H. Xu, H. J. Bart, C. Janiak, S. Henninger, G. Maurin, X. Zou and N. Stock, *Nat Commun*, 2019, **10**, 3025.
17. Z. Zhang, H. T. Nguyen, S. A. Miller, A. M. Ploskonka, J. B. DeCoste and S. M. Cohen, *J Am Chem Soc*, 2016, **138**, 920-925.
18. M. F. De Lange, J.-J. Gutierrez-Sevillano, S. Hamad, T. J. H. Vlugt, S. Calero, J. Gascon and F. Kapteijn, *J Phys Chem C*, 2013, **117**, 7613-7622.
19. S. Wang, J. S. Lee, M. Wahiduzzaman, J. Park, M. Muschi, C. Martineau-Corcos, A. Tissot, K. H. Cho, J. Marrot, W. Shepard, G. Maurin, J.-S. Chang and C. Serre, *Nat Energy*, 2018, **3**, 985-993.
20. W. Xu and O. M. Yaghi, *ACS Cent Sci*, 2020, **6**, 1348-1354.
21. M. J. Kalmutzki, C. S. Diercks and O. M. Yaghi, *Adv Mater*, 2018, **30**, e1704304.
22. S. Oien-Odegaard, B. Bouchevreau, K. Hylland, L. Wu, R. Blom, C. Grande, U. Olsbye, M. Tilset and K. P. Lillerud, *Inorg Chem*, 2016, **55**, 1986-1991.
23. N. M. Padial, E. Quartapelle Procopio, C. Montoro, E. Lopez, J. E. Oltra, V. Colombo, A. Maspero, N. Masciocchi, S. Galli, I. Senkovska, S. Kaskel, E. Barea and J. A. Navarro, *Angew Chem Int Ed Engl*, 2013, **52**, 8290-8294.
24. F. Fathieh, M. J. Kalmutzki, E. A. Kapustin, P. J. Waller, J. Yang and O. M. Yaghi, *Sci Adv*, 2018, **4**, eaat3198.
25. This study, where halide ions are ion-paired & not hydrogen-bonded to aqua ligands already present on nodes is different from the study by Dinca group (*J Am Chem Soc*, 2019, **141**, 13858) where the chemical identity of node-ligated anions, and therefore, the chemical identity of the MOF, is systematically varied. The Dinca group is looking at coordination-sphere effects; we are looking at first- (aqua vs. hydroxo), second- (halide-ion interacting with aqua ligands), and perhaps third-coordination-sphere effects (halide-ion interacting with water clusters that fill the mesopore).
26. J. Canivet, A. Fateeva, Y. Guo, B. Coasne and D. Farrusseng, *Chem Soc Rev*, 2014, **43**, 5594-5617.

27. A. M. Wright, A. J. Rieth, S. Yang, E. N. Wang and M. Dinca, *Chem Sci*, 2018, **9**, 3856-3859.
28. D. Yang, M. A. Ortuno, V. Bernales, C. J. Cramer, L. Gagliardi and B. C. Gates, *J Am Chem Soc*, 2018, **140**, 3751-3759.
29. J. Liu, Z. Li, X. Zhang, K.-i. Otake, L. Zhang, A. W. Peters, M. J. Young, N. M. Bedford, S. P. Letourneau, D. J. Mandia, J. W. Elam, O. K. Farha and J. T. Hupp, *ACS Catal*, 2019, **9**, 3198-3207.
30. Y. Yang, X. Zhang, S. Kanchanakungwankul, Z. Lu, H. Noh, Z. H. Syed, O. K. Farha, D. G. Truhlar and J. T. Hupp, *J Am Chem Soc*, 2020, **142**, 21169-21177.
31. J. Liu, Z. Lu, Z. Chen, M. Rimoldi, A. J. Howarth, H. Chen, S. Alayoglu, R. Q. Snurr, O. K. Farha and J. T. Hupp, *ACS Appl Mater Interfaces*, 2021, **13**, 20081-20093.
32. Y. Liao, T. Sheridan, J. Liu, O. Farha and J. Hupp, *ACS Appl Mater Interfaces*, 2021, **13**, 30565-30575.
33. F. Drache, F. G. Cirujano, K. D. Nguyen, V. Bon, I. Senkovska, F. X. Llabrés i Xamena and S. Kaskel, *Cryst Growth Des*, 2018, **18**, 5492-5500.
34. MOF-808-Cl and MOF-808-I behave similarly, but with slightly more capacity fade. See Figure 4e and SI.
35. X. Liu, X. Wang and F. Kapteijn, *Chem Rev*, 2020, **120**, 8303-8377.
36. H. E. Unland, P. R. Houser, W. J. Shuttleworth and Z.-L. Yang, *Agr Forest Meteorol*, 1996, **82**, 119-153.
37. F. Yang, Q. He, J. Huang, A. Mamtimin, X. Yang, W. Huo, C. Zhou, X. Liu, W. Wei, C. Cui, M. Wang, H. Li, L. Yang, H. Zhang, Y. Liu, X. Zheng, H. Pan, L. Jin, H. Zou, L. Zhou, Y. Liu, J. Zhang, L. Meng, Y. Wang, X. Qin, Y. Yao, H. Liu, F. Xue and W. Zheng, *B Am Meteorol Soc*, 2020, **102**, E1172-E1191.